Journal of
Composites Science

MDPI

Article

Structural Response of Thin-Web Beams to Various Web Opening Retrofit Techniques

Oday A. Salih *, Kaythar A. Ibrahim, Mohammed H. Shukur, Suhaib Y. K. Al-Darzi * and Sofyan Y. Ahmed

Civil Engineering Department, College of Engineering, University of Mosul, Mosul 41001, Iraq; kaythar6871@uomosul.edu.iq (K.A.I.); m.h.alkafaf@uomosul.edu.iq (M.H.S.); sofyan1975@uomosul.edu.iq (S.Y.A.)

* Correspondence: odaycivileng@uomosul.edu.iq (O.A.S.); suhaib.qasim@uomosul.edu.iq (S.Y.K.A.-D.)

Abstract

Accidental web openings caused by impact, corrosion, or conflict-related damage can substantially reduce the strength, stiffness, and stability of steel bridge girders. Although numerous studies have examined beams containing intentionally designed web openings, limited experimental research has systematically compared practical rehabilitation methods for accidental openings in slender-web plate girders. This study experimentally and numerically evaluates several rehabilitation configurations incorporating welded patch plates and transverse stiffeners. Ten slender-web steel girder specimens, each 1800 mm long, 800 mm deep, and 300 mm wide, were tested under monotonic concentrated loading at mid-span. Nonlinear finite element models were also developed to qualitatively examine the principal deformation and instability trends. Relative to the control specimen, the untreated web opening reduced the ultimate load by approximately 43% and exhibited approximately 10% greater deflection at its respective ultimate load. One-sided and two-sided welded patch plates increased the ultimate load of the damaged specimen by approximately 22% and 26%, respectively. Transverse stiffeners increased the ultimate load by approximately 73% while exhibiting substantially lower ultimate-load deflections. The combined use of patch plates and transverse stiffeners provided the greatest improvement, increasing the ultimate load by approximately 101–123% relative to the untreated damaged specimen and substantially reducing lateral instability. The findings demonstrate that effective rehabilitation of slender-web girders requires not only restoration of the interrupted load path but also restraint of web instability.

Keywords: accidental web opening; steel girder rehabilitation; welded patch plate; transverse stiffeners; slender-web buckling

Check for updates

Academic Editor: Krishanu Roy

Received: 28 June 2026

Revised: 11 August 2026

Accepted: 13 August 2026

Published: 14 August 2026

Copyright: © 2026 by the authors. Licensee MDPI, Basel, Switzerland. This article is an open access article distributed under the terms and conditions of the Creative Commons Attribution (CC BY) license.

1. Introduction

Steel plate girders are widely used in bridges because of their high strength-to-weight ratio, ease of fabrication, and ability to span long distances [1]. In practice, openings may occur in the web of a steel girder to accommodate service requirements, to reduce self-weight, or unintentionally as a result of corrosion, accidental impact, blast loading, or conflict-related damage [2]. Regardless of their origin, such openings interrupt the natural stress flow through the web and may significantly reduce the stiffness, strength, and stability of the girder [3]. The structural behavior of steel plate girders containing web openings is strongly influenced by their opening geometry, as previous investigations have shown [4]. As the opening area increases, the structural behavior is expected to show decreases in load-carrying capacity and deflections; in addition, circular openings are preferable to rectangular openings because they demonstrate better structural behavior [5,6]. It was also noted that the opening geometry plays a major role in influencing stress concentration mechanisms of thin-walled structures with openings subjected to bending and shear stresses [7,8]. In this regard, different researchers have attempted to explore techniques that could improve the behavior of steel beams with web openings [9]. Li et al. [10] and Jiang et al. [6,11] investigated the effect of opening on the seismic behavior of steel members and proved that through appropriate detailing, considerable changes in behavior can be observed. Recently, Silwal et al. [12] suggested the use of CFRP sheets and cover plates to recover some portion of the lost capacity of steel beams with web openings. An investigation into the behavior of steel beams with large opening holes subjected to high stress loads has also been carried out by Al-Sultan and Al-Rifaie [13]; it was found that stiffness reinforcement in the opening region considerably enhanced the ability to withstand web buckling and impact loading. The phenomenon of local buckling continues to pose an important issue regarding the performance of thin-web steel components with openings. Heidarpour and Bradford [8] focused on the aspect of web slenderness limits and the local buckling of steel members under combined loading conditions [14]. It was established that web slenderness is a key factor that determines the initiation of local buckling and the ultimate load capacity of steel members. Jia et al. [15] considered the impact of local buckling on the structural performance of castellated and composite beam. Liang et al. [16] also evaluated web-post buckling characteristics of octagonal web openings in steel beams using finite element analysis. They showed that the critical failure mode greatly depends on these characteristics. The repair of structural failures in steel bridge girders has also been considered in the past few years. Salih et al. [17] analyzed the repair of Mosul's Second Bridge using experiments and simulations. They confirmed that the application of local strengthening techniques could efficiently eliminate stress concentrations to avoid early buckling in the damaged steel parts [18]. Although previous studies have investigated the influence of web openings and various strengthening methods, most have focused on intentionally fabricated service openings or individual retrofit techniques. Experimental studies that systematically compare practical rehabilitation strategies for accidental web openings in slender-web steel girders remain limited. In particular, the relative effectiveness of one-sided and two-sided welded patch plates, transverse stiffeners, and their combined application has not been adequately quantified under identical experimental conditions. Therefore, the present study provides a comprehensive experimental and numerical comparison of these rehabilitation techniques and evaluates their influence on strength recovery, stiffness, and instability behavior. The findings establish practical recommendations for the rehabilitation of Al-Hurriyah's damaged steel bridge girders and extend the current understanding of instability-controlled slender-web members.

The scientific contribution of this work lies in (i) experimentally evaluating accidental web openings representative of real bridge damage rather than designed service openings, (ii) providing the first systematic comparison of one-sided and two-sided welded patch plates used individually and in combination with transverse stiffeners for slender-web plate girders, (iii) identifying the influence of these repair techniques on load-carrying capacity and instability behavior, and (iv) using nonlinear finite element analysis to qualitatively examine the deformation patterns and instability mechanisms observed experimentally. These contributions establish practical recommendations for the rehabilitation of damaged steel bridge girders, beyond the qualitative conclusions available in previous studies.

2. Research Questions and Hypotheses

There is still little experimental data on the rehabilitation of unintentional gaps in slender-web bridge girders, especially where instability controls the structural response, despite the substantial literature on steel beams with web openings. Thus, the following research issues were intended to be addressed by the current study:

1. RQ1: For unintentional web openings in slender-web steel girders, do various rehabilitation methods offer noticeably different degrees of strength recovery?
2. RQ2: Regarding restoring stiffness and postponing instability, are two-sided welded patch plates much more effective than one-sided patch plates?
3. RQ3: Is there a synergistic improvement that goes beyond the individual contributions of each technology when transverse stiffeners and welded patch plates are combined?
4. RQ4: Which rehabilitation approach offers the best balance between improving stiffness, reducing lateral instability, and recovering strength?

The experimental program was developed to test the following research hypotheses:

H1. *The structural performance of girders containing accidental web openings depends not only on restoring the lost cross-sectional area but also on suppressing web instability.*

H2. *Transverse stiffeners contribute more effectively to restoring structural capacity than welded patch plates alone because they directly restrain local web buckling.*

H3. *Combining welded patch plates with transverse stiffeners provides a greater improvement than either strengthening technique used individually.*

H4. *Two-sided welded patch plates produce more uniform stress redistribution than one-sided patches and therefore achieve greater strength recovery.*

3. Objective of the Study

The present work addresses a significant issue that arose during the rehabilitation of the Al-Hurriyah Bridge, a crucial infrastructure in the city of Mosul, Iraq [17]. This bridge was originally constructed with composite variable-depth steel girders featuring slender webs with stiffeners spaced at 2 m intervals, which supported a reinforced concrete slab. The bridge has six continuous spans (arranged as 45, 57, 68, 68, 57, and 45 m); the depth of steel girders varies from 1.9 to 3.4 m. The main 3.4 m depth section is fabricated with a 560 mm flange, with a 28 mm flange thickness and a 16 mm web thickness. The main steel girders and diaphragms of the Al-Hurriyah Bridge suffer from different levels of damage (Figure 1), where accidental opening occurred in the main girders and diaphragms, highlighting the need for practical rehabilitations. Bullets and explosives caused different sizes of irregular openings, which are the target of treatment during rehabilitation processes. Cutting and reshaping holes into a rectangular shape, using patch plates welded to one or two sides of the holes, or installing additional stiffeners around the holes were the main treatment strategies. The present work aimed to fabricate steel girder samples in the materials laboratory of the Civil Engineering Department, College of Engineering at the University of Mosul, considering the suggested opening treatment method. Accordingly, ten groups, each with one beam, were fabricated and tested. Three control beams without holes were fabricated: beams with stiffeners at the ends, beams without stiffeners at the ends, and beams with an additional two stiffeners at mid-span. An opening was established in each of the other seven beams, with different treatment configurations.

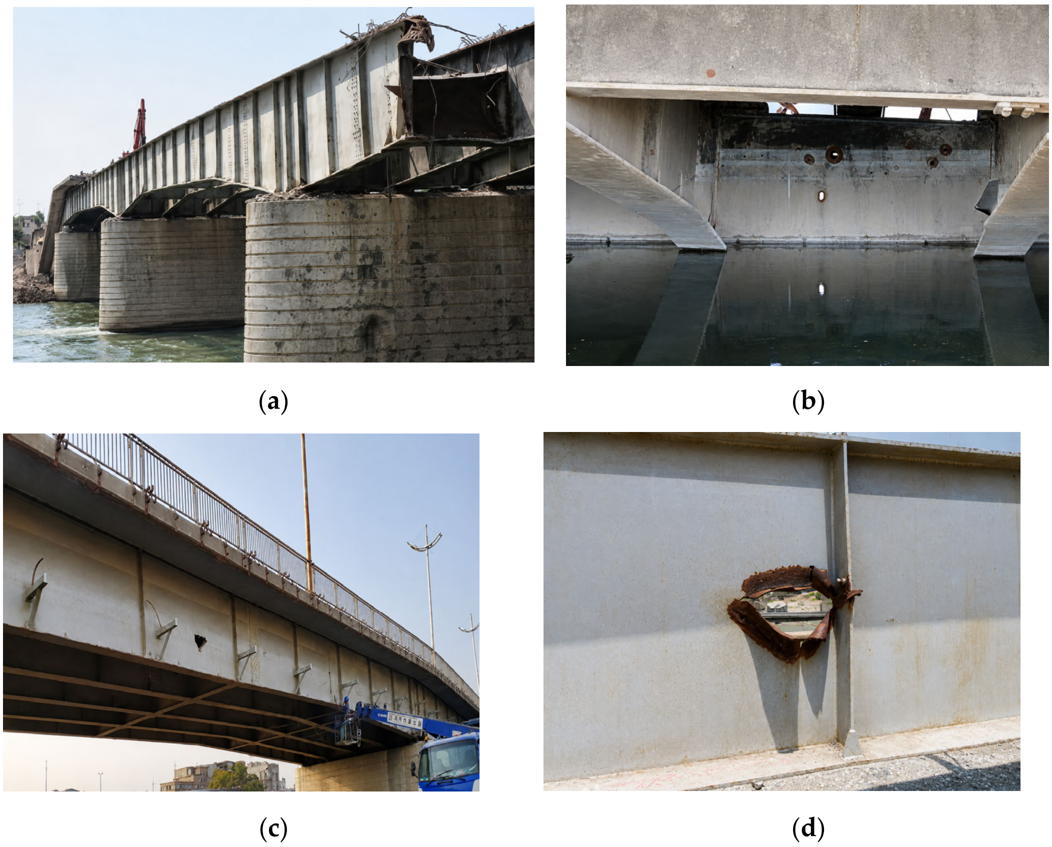

Figure 1. Types of damage to openings in the Al-Hurriyah Bridge. (**a**) Damage in bridge spans. (**b**) Opening in diaphragm. (**c**) Small opening in main girder. (**d**) Large opening in main girder.

All beams were tested using a concentrated monotonic load at mid-span. The experimental results were compared with those obtained from the control beams. The samples were modeled using the finite element method, and these modeling results were compared with the experimental results.

However, the experimental specimens were not intended to be a geometric scale model of the whole bridge; rather, they were intended to model the local response of damaged slender-web sections around accidental openings. Hence, the conclusions of this study primarily concern the effectiveness of the proposed repair technique at the component level. In the context of a full-scale assessment of bridges, the influence of composite action, continuity effects, traffic fatigue, corrosion, and actual boundary conditions should be examined separately. Accordingly, the objective of this study is not merely to demonstrate that strengthening improves the behavior of damaged girders; rather, the work seeks to experimentally evaluate competing rehabilitation strategies and verify the hypothesis that instability-controlled slender-web girders require repair techniques capable of restoring both load transfer and out-of-plane stability. Particular attention is devoted to quantifying the relative effectiveness of one- and two-sided welded patch plates, transverse stiffeners, and their combined application.

The experimental specimens were not intended to be a geometric scale model of the prototype bridge. Instead, they were designed to reproduce the governing local response of slender-web plate girders containing accidental web openings. The specimen proportions, web slenderness, loading arrangement, and boundary conditions were selected to ensure that web instability remained the dominant failure mechanism, thereby allowing a realistic evaluation of the proposed rehabilitation techniques.

4. Experimental Work

The present work includes testing 10 steel specimens with a length of 1800 mm, a depth of 800 mm, bf = 300 mm, tf = 10 mm, and tw = 4 mm. The span-to-depth ratio of the specimens was deliberately set to 2.25 to highlight the effect of the web opening on shear transfer, local buckling, and stability behavior. Because the main goal of this study was the investigation of rehabilitation methods for web openings in slender-web girders, it was important to design the specimens in such a way as to ensure web-controlled behavior instead of simple flexural yielding. A description of the investigated specimens with the different types of opening strengthening and rehabilitation is shown in Table 1. The beams were fabricated from plates purchased from local markets and welded with E70XX by a qualified welder. Two strips from the web and flanges of the steel beam were tested using a uniaxial tensile test according to ASTM specification [19], and the results are shown in Table 2 and Figure 2. This figure presents the tensile test results of the steel materials used in the specimens. The results confirm that the steel properties are consistent with A36 structural steel. The beam's dimensions and shapes are shown in Figures 3 and 4. Figure 3 shows the geometry and strengthening configurations adopted in the experimental program. The figure highlighted the differences between the controls and opened and retrofitted specimens. In addition, Figure 4 presents photographs of the fabricated specimens before testing, confirming the quality of the fabrication and the adopted repair details. The three control specimens with different initial boundary conditions (BC—a control beam with two side stiffeners, BC_NS—a beam without side stiffeners, and BC_TS—a beam with two stiffeners at mid-span) are adopted (Figure 3a,b,c, respectively). Because of the cost and complexity associated with fabricating and testing large-scale steel girder specimens, one representative specimen was adopted for each rehabilitation configuration to enable a comprehensive comparison of the proposed repair techniques. However, the BC-NS specimen was used solely as a reference to compare the experimental findings with theoretical results and does not represent an arrangement suitable for bridge construction, where transverse stiffening is always provided in support areas and at locations of loading. The opening size is 180 × 180 mm, and it was placed in the middle of the beam fabricated for specimen BO, as shown in Figure 3d. Two rehabilitation configurations were adopted using patch plates and intermediate stiffeners. The patch plates were fabricated using 6 mm thick steel plates and welded by using 3 mm E70XX fillet welding around the patch perimeter. The fabrication tolerance was maintained within ±1 mm for all steel parts. The first rehabilitation configuration was conducted using a patch plate of 190 × 190 mm, fixed by E70XX fillet welding on one and two sides of the beams (considering the effect of patch plate thickness), with side stiffeners for specimens BO_OP and BO_TP, as shown in Figure 3e,f, respectively. The second rehabilitation configuration was conducted using intermediate stiffeners at mid-span, without a patch plate, and with a patch plate fixed by welding on one and two sides for the beams with side stiffeners, designated as specimen BO_TS, BO_TS_OP, and BO_TS_TP, as shown in Figure 3g,h,i, respectively. Finally, the beam without side stiffeners was rehabilitated using two patch plates on each side, as shown in Figure 3j. The opening size of 180 × 180 mm was selected to represent severe local web damage while maintaining sufficient surrounding material for practical rehabilitation using welded patch plates and transverse stiffeners. The retrofit configurations were chosen based on practical repair techniques adopted during bridge rehabilitation and to enable a systematic comparison between one-sided and two-sided patch plates, transverse stiffeners, and their combined application under identical test conditions. The specimens were tested using a point load at mid-span, where Figure 5 illustrates the loading arrangement and instrumentation used during testing and ensuring consistent boundary conditions for all specimens. The hydraulic jacks (Zhengzhou Lead

Equipment Co., Zhengzhou, China) with a 2000 kN load cell were used in the test. The test was conducted using a monotonic load with a 0.1 kN/sec loading rate. The deflection and lateral displacement were measured during the test using calibrated LVDTs connected to the data logger, and the data were transferred to the computer. The Material Engineering Laboratory calibrates all instruments used in tests in the Civil Engineering Department, College of Engineering at the University of Mosul, which holds an ISO 17025 certificate [20]. The test continued until significant buckling or effective distortion of the beams was reached (Figure 6). No lateral constraints were applied externally during the tests. This strategy was deliberately chosen to allow instability to emerge on the lateral side and to assess the efficacy of the new rehabilitation procedures under similar conditions. The figure clearly shows the typical failure mode observed during testing. The failure was dominated by web buckling and overall instability rather than material yielding. The exact loading condition was used for all specimens. The failure of the beams was due to the instability of the member. The failure modes are characterized by distortion of the specimens with unequal horizontal displacements and are accompanied by local buckling in the web. To keep things consistent, the failure load for each sample was taken to be the maximum load reached before any of the following happened: a reduction in the load, visible web buckling, a sharp increase in lateral deflection, gross deformation of the beam, or the inability of the sample to support any further loads without becoming unstable. The load reached would thus be the sample's instability failure load, not the actual material failure load. Meanwhile, measuring deflection was the primary control for determining the beam condition, and the beam's distortion helped define the failure condition. The results are then plotted as load–displacement and load–lateral displacement curves.

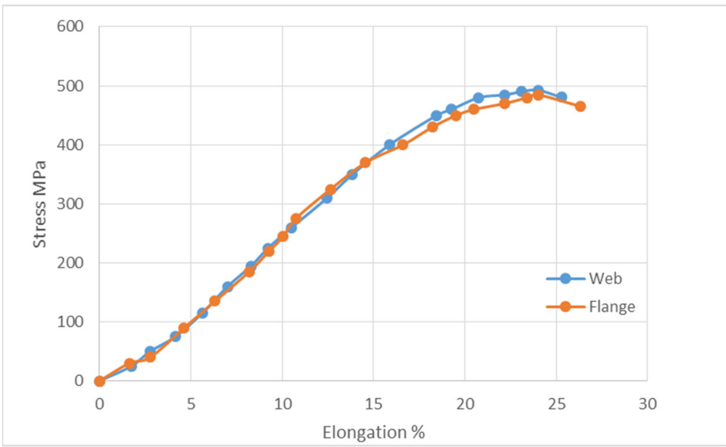

Figure 2. Steel section uniaxial tensile test results. These stress–strain relationships were used to determine the material properties considered in the FEA, such as the yield strength, ultimate tensile strength, and elastic modulus.

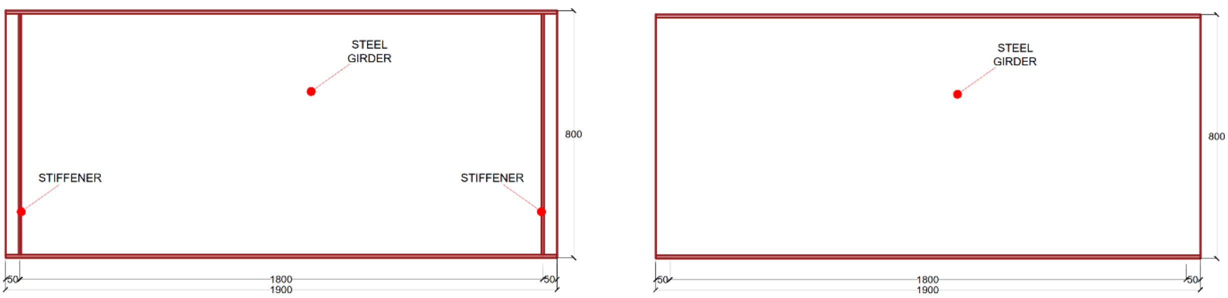

(**a**) (**b**)

Figure 3. *Cont.*

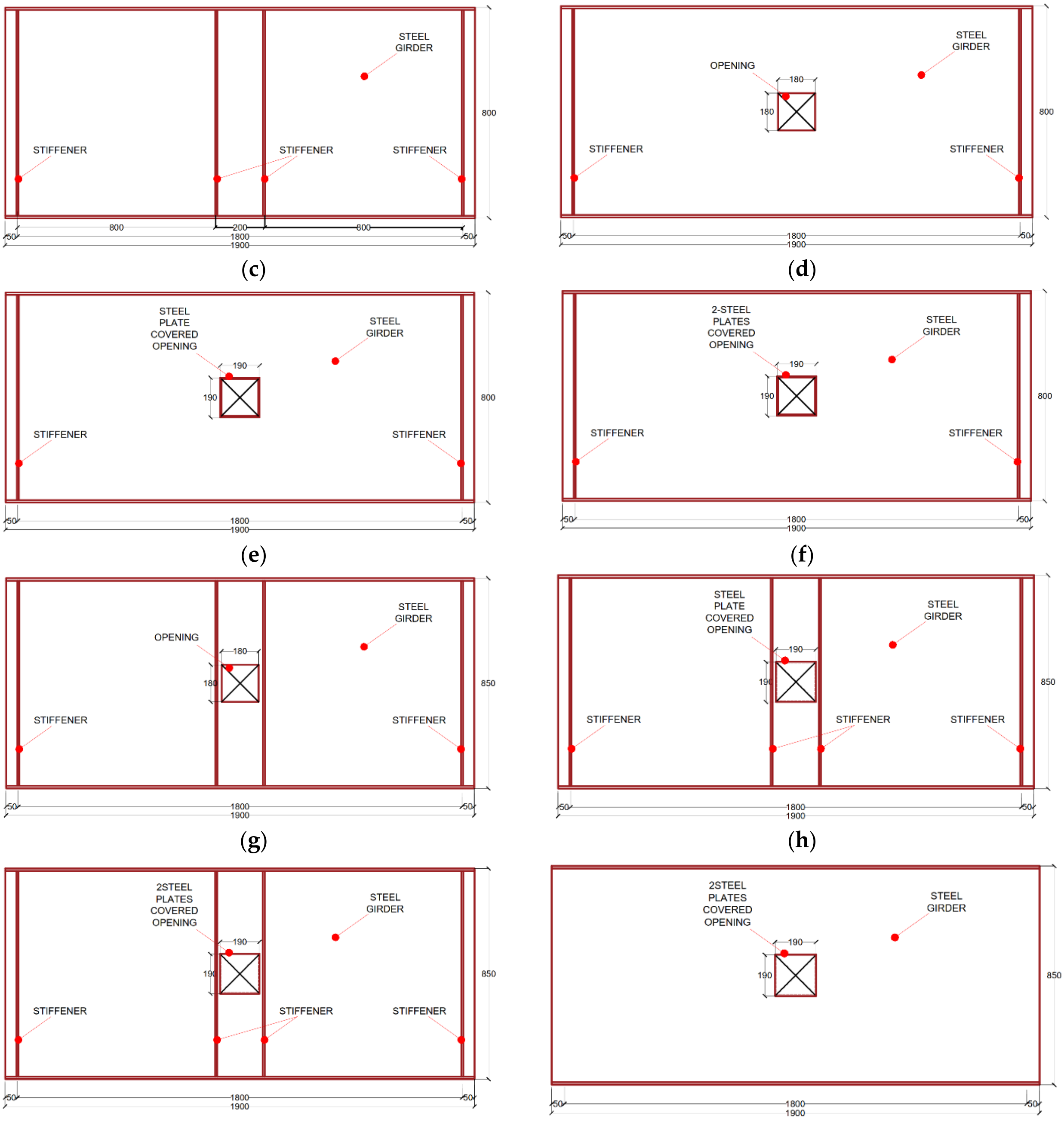

Figure 3. Configuration and dimensions of specimen drawings. (**a**) BC. (**b**) BC_NS. (**c**) BC_TS. (**d**) BO. (**e**) BO_OP. (**f**) BO_TP. (**g**) BO_TS. (**h**) BO_TS_OP. (**i**) BO_TS_TP. (**j**) BO_NS_TP.

(**a**) (**b**)

Figure 4. *Cont.*

(c) (d) (e) (f) (g) (h) (i) (j)

Figure 4. Images of specimen configurations. (**a**) BC beam control (no opening). (**b**) BC_NS beam control with no stiffeners at ends. (**c**) BC_TS beam control strengthening by two stiffeners at mid-span. (**d**) BO beam with opening of 180 × 180 mm at mid-span. (**e**) BO_OP beam with opening of 180 × 180 mm at mid-span retrofitted by one side patch plate. (**f**) BO_TP beam with opening of 180 × 180 mm at mid-span retrofitted by two side patch plates. (**g**) BO_TS beam with opening of 180 × 180 mm at mid-span retrofitted by two stiffeners. (**h**) BO_TS_OP beam with opening of 180 × 180 mm at mid-span retrofitted by two stiffeners and one patch plate. (**i**) BO_TS_TP beam with opening of 180 × 180 mm at mid-span retrofitted by two stiffeners and two patch plates. (**j**) BO_NS_TP beam with opening of 180 × 180 mm at mid-span with no stiffeners at ends retrofitted by two side patch plates.

Table 1. Designations and descriptions of steel beam specimens.

No.	Designation	Description
1	BC	Beam control (no opening).
2	BC_NS	Beam control with no stiffeners at ends.
3	BC_TS	Beam control strengthening by two stiffeners at mid-span.

Table 1. *Cont.*

No.	Designation	Description
4	BO	Beam with opening of 180 × 180 mm at mid-span.
5	BO_OP	Beam with opening of 180 × 180 mm at mid-span retrofitting by one side patch plate.
6	BO_TP	Beam with opening of 180 × 180 mm at mid-span retrofitting by two side patch plates.
7	BO_TS	Beam with opening of 180 × 180 mm at mid-span retrofitted by two stiffeners.
8	BO_TS_OP	Beam with opening of 180 × 180 mm at mid-span retrofitted by two stiffeners and one patch plate.
9	BO_TS_TP	Beam with opening of 180 × 180 mm at mid-span retrofitted by two stiffeners and two patch plates.
10	BO_NS_TP	Beam with opening of 180 × 180 mm at mid-span with no stiffeners at ends retrofitted by two side patch plates.

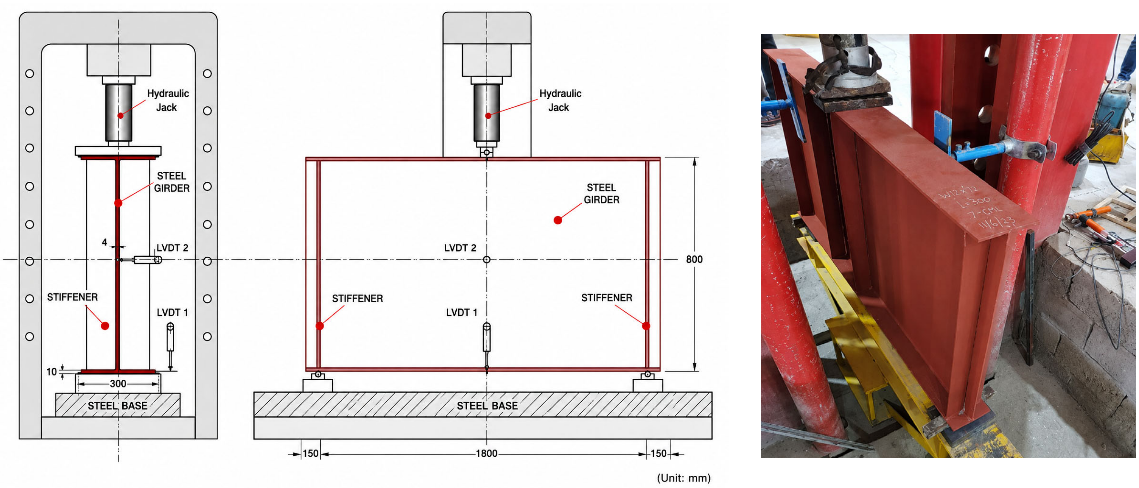

Figure 5. Specimen section dimensions and testing setting configuration.

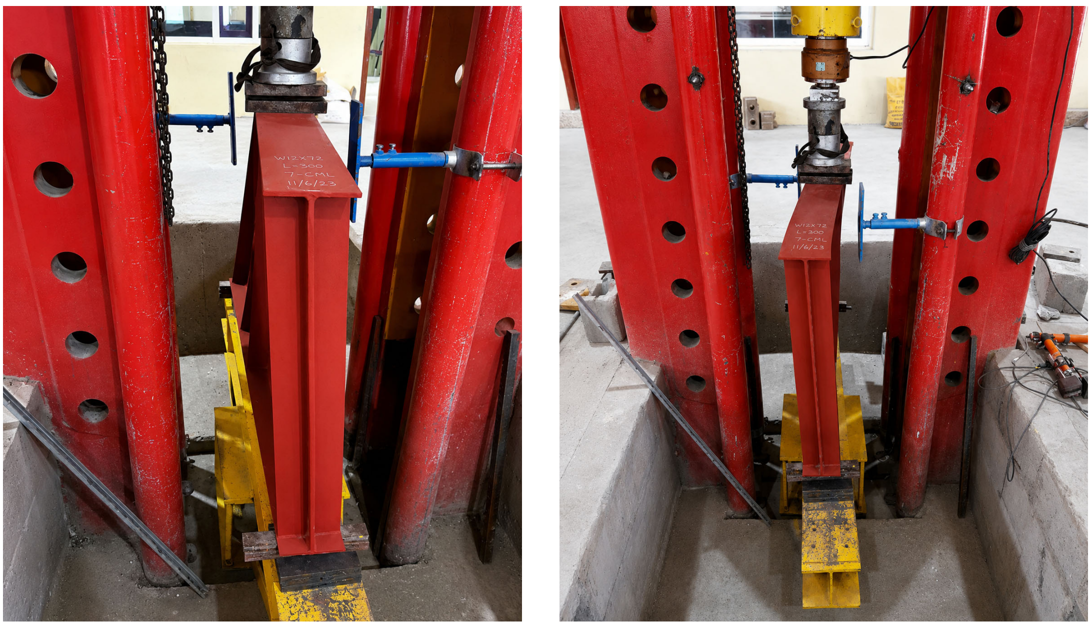

Figure 6. Specimen distortion during testing.

https://doi.org/10.3390/jcs10080429

Table 2. Steel beam strip test results.

Strip Location	Yield Stress fy (MPa)	Ultimate Strength fu (MPa)	Elongation (%)	Steel Type
Web	298.3	492.6	24	A36
Flange	286.7	484.9	25	A36

5. Theoretical and Numerical Work

5.1. AISC Strength Estimations

Initially, the resistance of the intact steel beam section was estimated using the available AISC provisions to provide a reference capacity with which to compare the experimentally tested opened and retrofitted beams. This work depends on the present beams having a slender web, considering the AISC limitations. According to the limitation of the AISC specification [21,22], the beam has a non-compact flange due to the following:

$$\lambda_f = b_f/2t_f = 300/2/(10) = 15 > \lambda_{pf} = 0.38(E/f_{yf})^{0.5} = 0.38(200000/286.7)^{0.5} = 10.04$$

But $\lambda_f = 15 < \lambda_{rf} = (E/f_{yf})^{0.5} = (200000/286.7)^{0.5} = 26.41$
In addition, the beam has a non-compact web due to the following:

$$\lambda_w = h/t_w = 780/4 = 195 > \lambda_{pw} = 3.76(E/f_{yw})^{0.5} = 3.76(200000/298.3)^{0.5} = 97.36$$

$$\lambda_w = h/t_w = 195 > \lambda_{rw} = 5.7\ (E/f_{yw})^{0.5} = 5.7(200000/298.3)^{0.5} = 147.59$$

where the material properties are as follows: f_{yf} = 286.7 MPa, f_{yw} = 298.3 MPa, and E = 200,000 MPa. The geometric properties of the welded I-section were independently recalculated based on the following measured dimensions: d = 800 mm, bf = 300 mm, tf = 10 mm, tw = 4 mm, and h = 780 mm. The results regarding the moment capacity of the beam after considering the lateral buckling were found by adopting Equation (1) to find the critical stress (Fcr) and the resisting moment (MR) calculated from Equation (2) [23]. A flexural stability check was also performed using the AISC provisions. The corresponding flexural resistance exceeded the governing slender-web shear-buckling capacity calculated below. Therefore, flexural resistance does not govern the theoretical capacity of the tested specimens.

$$\mathrm{Fcr} = \mathrm{Cb} * \pi^2 * \mathrm{E} * \left[1 + \frac{0.078 * J_c * \left(\frac{L_b}{r_{ts}}\right)^2}{S_x * h_o}\right]^{0.5} / \left(\frac{L_b}{r_{ts}}\right)^2 \quad (1)$$

$$M_R = \mathrm{Fcr} * \mathrm{Sx} \quad (2)$$

$$\mathrm{Presist.} = \frac{4 * M_R}{L} \quad (3)$$

The resulting properties are A = 9120 mm^2, Ix = 1.094384 × 10^9 mm^4, Iy = 4.500416 × 10^7 mm^4, Sx = 2.73596 × 10^6 mm^3, J = 2.1664 × 10^5 mm^4, ho = 790 mm, Cw = 7.02177 × 10^{12} mm^6, and rts = 80.61 mm. The previously reported value of 1.094 × 10^9 mm^4 corresponds to Ix rather than Iy. The elastic yielding moment based on the flange yield stress is My = Fyf ∗ Sx = (286.7)(2.73596 × 106) = 784.4 kN.m, corresponding to a central point load of Py = 4 ∗ My/L = 1743 kN. Therefore, flexural yielding does not govern the tested specimens. The governing theoretical capacity is controlled by slender-web shear buckling. The shear resistance can be calculated as follows:

$$\mathrm{Aw} = \mathrm{h} * \mathrm{tw} = 780 * 4 = 3120\ \mathrm{mm}^2$$

$$h/tw = 195 > 1.37\ (kv * E/fy)^{0.5} = 1.37\ (kv * E/fy)^{0.5} = 1.37\ (5.34 * 200{,}000/298.3)^{0.5} = 82$$

$$Cv = 1.51E * kv/((h/tw)^2 * fy) = 1.51 * 200{,}000 * 5.34/((780/4)^2 * 298.3) = 0.142$$

$$Vn = 0.6 * Fy * Aw * Cv \tag{4}$$

$$Vn = 0.6\ (298.3)\ (3120)\ (0.142) = 79.4\ \text{kN}$$

Using Aw = 3120 mm^2, h/tw = 195, kv = 5.34, and Cv = 0.142, the nominal shear strength is Vn = 79.4 kN. Since the support reaction under a central point load is P/2, the corresponding governing theoretical concentrated load is Pn = 2 ∗ Vn = 158.8 kN. The maximum experimental load recorded was Pu = 155.54 kN, which corresponds to the support reaction of Vu = Pu/2 = 77.77 kN < nominal shear resistance Vn. The recalculated AISC strength evaluation indicates that flexural yielding does not govern the behavior of the tested slender-web beam. Instead, the theoretical capacity is controlled by web shear buckling, resulting in a governing concentrated load of approximately 159 kN. Therefore, the theoretical benchmark adopted in the following comparisons has been revised accordingly.

The patch plate and the weld were verified for an opening of 180 × 180 mm and a patch plate of 190 × 190 mm. Thus, the total weld perimeter was Lw = 4 ∗ 190 = 760 mm. The use of a 3 mm E70XX fillet weld provided the following resistance:

$$Rn = 0.6 * FEXX * (0.707 * w) * Lw \tag{5}$$

$$Rn = 0.6(483 * 0.707 * 3 * 760) = 467\ \text{kN}$$

Using a resistance factor of ϕ = 0.75, the design weld strength ϕRn = 350 kN, which is greater than the maximum force in the tested specimen. Therefore, no welding failure was expected, and none was observed during the tests.

Where the following was the case:

The cross sectional area A = 2 ∗ (bf ∗ tf) + tw ∗ h = 2 ∗ (300 ∗ 10) + (780 ∗ 4) = 9120 mm^2;

C_b—bending coefficient, $r^2_{ts} = (I_y * C_w)^{0.5}/S_x$, or $r^2_{ts} = I_y * h_w/(2 * S_x)$;

.. for doubly symmetric I-shapes with rectangular flanges;

C_w—warping constant or $C_w = I_y * h^2_w/4$;

.. for doubly symmetric I-shapes with rectangular flanges;

S_x—section modulus about the major axis = 2.736 × 10^6 mm^3;

E—modulus of elasticity of steel, J—torsional constant;

I_x—moment of inertia about the major axis = 1.094 × 10^9 mm^4;

I_y—moment of inertia about the minor axis = 4.5 × 10^7 mm^4;

C = 1.0 .. for doubly symmetric I-shapes, h_o—distance between flanges' centroid;

Kv = 5.34, Presist. = resisting load, L—span of the beam [21,22].

The bearing and local yielding effects were minimized by using end stiffeners and a loading plate at the point of application. No local flange crippling, web bearing failure, or weld fracture was observed during testing. The dominant failure mode was global instability, accompanied by web buckling and lateral deformation, confirming that slender-web behavior governed the specimens' response.

5.2. Finite Element Analysis

The study also included a beam simulation using the finite element program ANSYS, 2024R and 2025R [24]. Four models were adopted to simulate the specimen: (1) BC, representing the control beam without an opening; (2) BC-TS, the controlled beam strengthened by two stiffeners in the middle; (3) BO, the controlled beam with an opening; and (4) BO-TS, the beam with an opening treated by adding two stiffeners at the middle. The finite element models were also used to investigate the effect of using another rehabilitation method such as horizontal stiffeners at the top and bottom of the opening and the vertical stiffeners used in the BO-TS model. Figure 7 presents the finite element models developed in ANSYS. The models were used to investigate the influence of opening and stiffening details on structural behavior. The finite element analysis used the three-dimensional four-node Shell 181 element. The SHELL181 is a four-node shell element with six degrees of freedom per node, capable of representing both membrane and bending behavior. The element is well suited for nonlinear analysis of thin- and moderately thick-walled steel structures because it incorporates geometric and material nonlinearities, including large deflection and plasticity effects [24]. A three-dimensional model consists of a maximum number of (1566) nodes, connecting (1424) elements. The boundary conditions simulated by restraint of the three degrees of freedom (Ux, Uy, and Uz) in one node at the bottom of the side of the beam, with the restraint of (Ux and Uz) on the other side of the beam as shown in Figure 7. These idealized nodal restraints were intended to reproduce the nominal simply supported test arrangement. However, re-examination of the numerical results indicated that the idealized representation of the support and loading conditions may influence the predicted instability load, particularly for the unstiffened control specimen BC. Therefore, the numerical model is not considered quantitatively validated for prediction of the ultimate load. The large displacement option with 1000 sub steps was chosen for the analysis, with a nonlinear option adopting convergence criteria of 0.01 for the termination of the analysis processes. The material properties used in the finite element analysis are stated in Table 3. The nonlinear analysis used the inelastic bilinear isotropic hardening (BISO) model [24,25]. To evaluate the sensitivity of the numerical response to the assumed post-yield constitutive behavior, analyses were performed using tangent moduli of Et = 8000 MPa and Et = 120,000 MPa. The value Et = 8000 MPa was adopted as the reference material model. The higher value of 120,000 MPa was used only as a sensitivity/calibration case and is not considered representative of the post-yield behavior of A36 steel. Accordingly, results obtained using Et = 120,000 MPa are presented only to demonstrate the sensitivity of the numerical prediction to the constitutive assumption and are not used for quantitative parametric conclusions. A limited mesh-sensitivity assessment was performed using uniform mesh sizes of 100 $\times$ 100 mm and 50 $\times$ 50 mm. The 50 $\times$ 50 mm mesh was retained for the numerical analyses to provide greater spatial resolution of the local web response. Because only two mesh sizes were investigated, this comparison is not presented as a formal mesh-convergence study. Accordingly, no claim of mesh-independent ultimate-load prediction is made, consistent with the use of the finite element model primarily for qualitative interpretation. The ANSYS program uses the Newton–Raphson solution technique in the nonlinear analysis of the model meshed using a uniform mesh size of 50 mm in all directions for web, flanges, and stiffeners. Geometrical imperfections in the initial step were introduced as out-of-plane deflection of the web plate to most naturally induce buckling. Residual stresses resulting from fabrication and welding were not explicitly considered in the finite element model. The primary objective of the numerical analysis was to provide a consistent comparative assessment of the different rehabilitation configurations rather than to reproduce every aspect of the fabrication process. Accordingly, identical modeling assumptions were adopted for all specimens, allowing the influence of the repair techniques to be isolated. The patch plate was treated as the shell plate, with the same characteristics as the web plate; ties around the plate approximated the weld. Loading and support plates were introduced to prevent artificial stress concentration in the numerical simulation. In the numerical model, the welded patch plates were assumed to be perfectly connected to the web using bonded shell connections. The weld geometry and welding process were not modeled explicitly, and welding-induced residual stresses and heat-affected zone effects were neglected. This simplification is considered reasonable because the objective of the finite element analysis was to evaluate the comparative structural response of the rehabilitation techniques rather than to reproduce the exact local behavior of the welded joints.

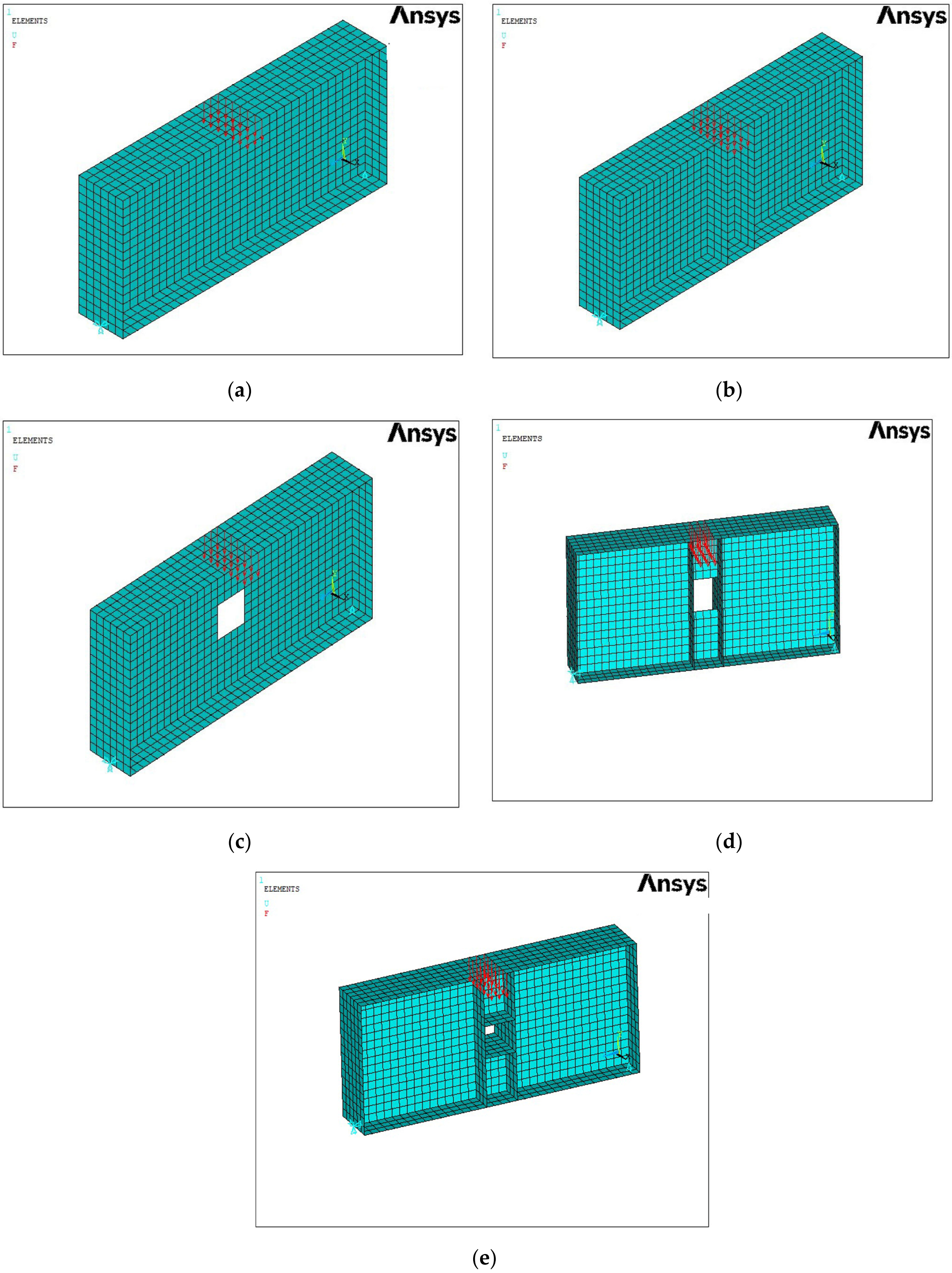

Figure 7. The models used in finite element analysis. (**a**) BC finite element model. (**b**) BC-TS finite element model. (**c**) BO finite element model. (**d**) BO-TS finite element model. (**e**) BO-TS finite element model with additional horizontal stiffeners.

Table 3. Steel beam properties used in finite element analysis.

Yield Stress fy (MPa)	Modulus of Elasticity (MPa)	Poisson's Ratio	Tangent Modulus of Elasticity (MPa)
298	200,000	0.3	8000

Four representative specimens were selected for numerical comparison to capture the principal structural conditions investigated in this study: the intact girder BC, the stiffened intact girder BC_TS, the damaged girder containing a web opening BO, and the rehabilitated girder strengthened with transverse stiffeners BO_TS. The experimental and numerical ultimate loads were compared to assess the predictive capability and limitations of the adopted numerical model. Using the reference bilinear material model with Et = 8000 MPa, the predicted ultimate loads of BC and BO were 49.85 and 32.50 kN, respectively, compared with experimental values of 121.2 and 69.6 kN. These values correspond to under-predictions of approximately 59% and 53%, respectively. In contrast, considerably closer agreement was obtained for the stiffened specimens BC_TS and BO_TS. Because a similarly large discrepancy occurs for the intact specimen BC, which contains no web opening, the disagreement cannot be attributed solely to geometric imperfections or local distortions around the opening. The comparison indicates that the predicted instability load is sensitive to the numerical idealization of the test arrangement, including the support and loading boundary conditions, initial geometric imperfections, residual stresses, and the adopted constitutive representation. Consequently, the present finite element model is retained as a qualitative tool for examining deformation patterns and instability trends rather than as a quantitatively validated predictor of ultimate load, although it is less accurate in predicting the absolute capacity of highly imperfection-sensitive specimens [26,27]. Although quantitative differences were observed between the experimental and numerical ultimate loads, the finite element model successfully reproduced the overall structural behavior, deformation characteristics, and the relative influence of the investigated rehabilitation techniques. The numerical model represents an idealized structural system in which fabrication tolerances, welding-induced residual stresses, initial geometric imperfections, and local material variability were not explicitly considered. Consequently, the numerical analysis is retained primarily as a qualitative aid for interpreting deformation patterns, stress redistribution, and instability mechanisms rather than as a quantitatively validated predictor of ultimate load.

6. Results and Discussion

The results of the ten specimens regarding deflection and lateral displacements with the applied loads are listed in Table 4. The experimental results (ultimate loads, deflection, and lateral displacement) differ from those obtained from the control beam (BC). The results regarding applied loads versus displacements are also plotted and shown in Figure 8, which demonstrates that the opening significantly reduced stiffness and load-carrying capacity. At the same time, patch plates and stiffeners improved the structural response. Figure 9 also indicates that the retrofitting methods reduced lateral displacement and delayed instability compared with the specimen containing an untreated opening.

The results of control beam BC listed in Table 4 showed a difference in ultimate load compared with those obtained by AISC specification calculation. The experimental ultimate load obtained was 121.2 kN, which was approximately 24% lower than the governing AISC theoretical capacity of 159 kN. The results listed in Table 4 showed the variation between the results of the tested beams. The first target is to understand the effect of the presence of a hole in the BO specimen, which reduces the ultimate strength by about 43%, increases the deflection by about 10%, and increases the lateral displacement by 1% compared with the control specimen BC. It should be noted that the reported deflection percentages correspond to the deflection measured at the ultimate load of each specimen and therefore reflect the combined effects of stiffness and load-carrying capacity rather than stiffness alone. The opening interrupted the natural shear flow path through the web, producing stress concentrations around the opening corners and reducing the effective shear-resisting area. The resulting increase in local stresses accelerated web buckling and reduced the overall stability of the slender-web girder, leading to the observed reduction in ultimate load. The results also showed that adding two stiffeners in the middle of beams for specimen BC_TS would increase the ultimate resistance by about 23% and decrease the deflection and lateral displacement by about 42% and 40%, respectively. Meanwhile, the ultimate load decreased by about 40% when the side stiffeners were eliminated in specimen BC_NS. Figure 8 showed that the deflection against the load 72.5 kN for specimen BC was (1.0 mm), which is less than the deflection obtained in BC_NS, of about 39%; furthermore, the lateral displacement obtained from Figure 9 for specimen BC against the load of 72.5 kN was (2.9 mm), which is also less than the deflection obtained in BC_NS of about 71%. To understand the effect of the different methods adopted in treating the hole in the specimens, the results of the beam with a hole at mid-span were listed in Table 5, with percentage differences compared with BO specimens. The results showed that the ultimate load was raised using patch plates with about 22% and 26% for specimens BO_OP and BO_TP, respectively, compared with the BO specimen. Meanwhile, deflection was reduced at the ultimate stage, compared with the BO specimen, by about 8% and 1% for specimens BO_OP and BO_TP, respectively. A significant effect was noticed in ultimate resistance when an additional two stiffeners were used at the middle of the beam; ultimate resistance increased for BO_TS by about 73% compared with the BO specimen; at the same time, the deflection and lateral displacement at the ultimate stage decreased by about 68% and 45%, respectively. The substantial increase in strength provided by the transverse stiffeners is primarily attributed to the restraint they provide against out-of-plane deformation of the slender web. The stiffeners increase the local flexural rigidity of the web panel surrounding the opening, thereby delaying the initiation of local buckling and allowing the web to continue transmitting shear forces more effectively. In addition, the stiffeners shorten the effective buckling length of the web panel, resulting in improved stability and increased load-carrying capacity. An additional increase in ultimate strength was shown using patch plates from one and two sides, which were about 101% and 123%, respectively. It can be shown from Figure 8 that the deflections for BO_TS_OP and BO_TS_TP against an ultimate load of 69.6 kN were 0.42 and 0.6 mm, respectively, which is less than for the BO specimen (about 89% and 84%, respectively). Furthermore, the lateral displacements shown in Figure 9 decreased to 1.9 and 1.7 mm for specimens BO_TS_OP and BO_TS_TP, respectively, against an ultimate load of 69.6 kN for specimen BO, representing 77% and 79.5%, respectively. It can be clearly shown that the welded patch plates partially restored the interrupted load path around the opening by increasing the effective shear transfer area of the web. However, because the patch plates alone provided limited restraint against out-of-plane deformation, local web instability remained the governing mechanism. Consequently, the improvement in strength was less pronounced than that achieved using transverse stiffeners.

Table 6 compares the experimental results and the governing AISC theoretical capacity of approximately 159 kN controlled by slender-web shear buckling. Most specimens reached lower ultimate loads because their behavior was governed by instability and excessive deformation. Specimen BO_TS_TP showed the closest agreement with the theoretical value, with a difference of approximately 2%, whereas the BC and BO specimens were approximately 24% and 56% below the theoretical capacity, respectively. Although specimen BO_TS_TP exhibited a slightly higher ultimate load than the undamaged stiffened control specimen BC_TS, and its measured lateral displacement was marginally greater than that of BO_TS_OP, these differences are relatively small considering that only one specimen was tested for each rehabilitation configuration. Consequently, such variations may partly reflect normal experimental scatter associated with fabrication tolerances, welding, material variability, and measurement un-certainty. Therefore, the conclusions of the present study are based on the overall behavioral trends of the investigated rehabilitation techniques rather than on isolated differences between individual specimens.

Table 4. Experimental results and percentage differences relative to the control specimen (BC).

No.	Designation	Pu kN	Pu %Diff. with BC	Deflection Ult. mm	Deflection %Diff. with BC	Lateral Displacement Ult. mm	Lateral Displacement Diff. Relative to BC (%)
1	BC	121.2	0	3.47	0	8.22	0
2	BC_NS	72.5	−40	1.39	−60	14.57	77
3	BC_TS	149.1	23	2.01	−42	4.97	−40
4	BO	69.6	−43	3.83	10	8.32	1
5	BO_OP	84.9	−30	3.53	2	6.29	−23
6	BO_TP	87.6	−28	3.81	10	5.97	−27
7	BO_TS	120.2	−1	1.22	−65	4.57	−44
8	BO_TS_OP	140.05	16	2.02	−42	3.46	−58
9	BO_TS_TP	155.54	28	2.01	−42	4.72	−43
10	BO_NS_TP	72.6	−40	3.3	−5	14.56	77

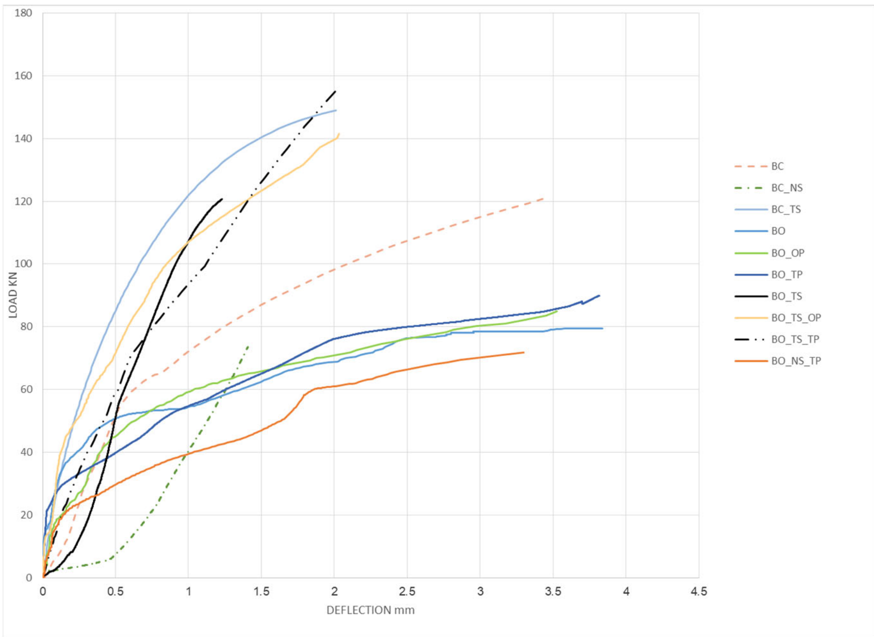

Figure 8. The load–deflection curves obtained from the experimental tests.

The lateral displacement, which represents the buckling of the web listed in Table 4, showed that the web buckling was greatly affected by the presence of lateral stiffeners. The buckling increased by about 77% for BC_NS and BO_NS_TP compared with the BC specimen despite the presence of the patch plate in the last one—recall that only 60% of the ultimate resistance was gained in those specimens. Meanwhile, the opening in the BO specimen slightly increased the buckling by about 1% compared with the control specimen BC. However, the expected results gained from using additional stiffeners at the middle were as follows: buckling was reduced by about 40%, 44%, 58%, and 43% for specimens BC_TS, BO_TS, BO_TS_OP, and BO_TS_TP, respectively, compared with the BC specimen.

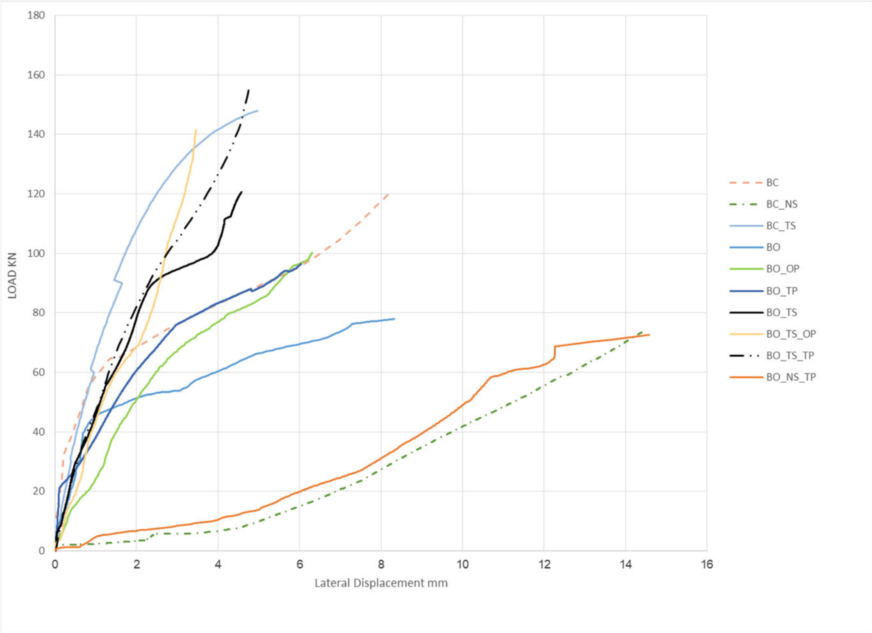

Figure 9. The load–lateral displacement curves obtained from the experimental tests.

Table 5. Ultimate load, ultimate deflection, and ultimate lateral displacement results for specimens with a hole at mid-span, and percentage improvement of rehabilitated specimens relative to the untreated specimen (BO).

No.	Designation	Pu kN	Pu %Diff. with BO	Deflection Ult. mm	Deflection %Diff. with BO	Lateral Displacement Ult. mm	Lateral Displacement Diff. Relative to BO %
1	BO	69.6	0	3.83	0	8.32	0
2	BO_OP	84.9	22	3.53	−8	6.29	−24
3	BO_TP	87.6	26	3.81	−1	5.97	−28
4	BO_TS	120.2	73	1.22	−68	4.57	−45
5	BO_TS_OP	140.05	101	2.02	−47	3.46	−58
6	BO_TS_TP	155.54	123	2.01	−48	4.72	−43

According to the results shown in Table 5, the lateral displacement of the BO specimen with the opening was reduced by using a patch plate at one and two sides by about 24% and 28% for BO_OP and BO_TP, respectively. It should be noted that the percentage values presented in Table 5 are calculated with respect to the untreated specimen containing the web opening (BO), whereas the percentages reported in Table 4 are referenced to the intact control specimen (BC). Consequently, the reported percentages are not directly comparable because they employ different reference specimens. These results indicate that the patch plate will reduce the web's buckling and enhance the beam's ultimate resistance. The usage of intermediate stiffeners in specimens with openings—BO_TS, BO_TS_OP, and BO_TS_TP—reduces the lateral displacements by about 45%, 58%, and 43%, respectively, compared with the BO specimen. Thus, the combined rehabilitation technique produced the greatest improvement because the two strengthening mechanisms acted simultaneously. The patch plates restored the local stress-transfer path across the damaged region, while the transverse stiffeners restrained web instability and redistributed the stresses over a larger portion of the web panel. This interaction delayed local buckling and enabled a more uniform stress distribution, resulting in a substantial increase in ultimate strength.

Table 6. Specimens' ultimate load results compared with the governing AISC slender-web shear-buckling capacity.

No.	Designation	Pu kN	Difference from Governing AISC Capacity, Pn = 159 kN (%).
1	BC	121.2	−24
2	BC_NS	72.5	−54
3	BC_TS	149.1	−6
4	BO	69.6	−56
5	BO_OP	84.9	−47
6	BO_TP	87.6	−45
7	BO_TS	120.2	−24
8	BO_TS_OP	140.05	−12
9	BO_TS_TP	155.54	−2
10	BO_NS_TP	72.6	−54

However, the retrofitting method did not alter the failure modes of the beams. Still, it decreased the amount of deflection and lateral displacement compared with the control specimen. The experimental observations demonstrate that the effectiveness of a rehabilitation technique depends not only on restoring the removed steel area but also on controlling instability. The results indicate that the structural response of slender-web girders is governed primarily by web buckling rather than material yielding. Consequently, rehabilitation methods capable of simultaneously restoring the load-transfer path and restraining out-of-plane deformation provide substantially greater improvements than techniques based solely on increasing the local cross-sectional area.

The finite element results are compared with the experimental responses in Figure 10 and Table 7. To examine the sensitivity of the numerical predictions to the adopted post-yield constitutive assumption, additional analyses were performed using the reference tangent modulus Et = 8000 MPa. Under this material model, the predicted ultimate loads of specimens BC and BO were 49.85 and 32.50 kN, respectively, compared with the corresponding experimental values of 121.2 and 69.6 kN. These results represent under-predictions of approximately 59% for BC and 53% for BO. In contrast, the numerical predictions for the stiffened specimens BC_TS and BO_TS were considerably closer to the experimental results. The large discrepancy observed for BC is particularly important because this specimen contains no web opening; therefore, the disagreement cannot be attributed solely to imperfection sensitivity or local distortion around an opening. The results indicate that the predicted instability response is sensitive to the idealization of the experimental system, including support and loading boundary conditions, initial geometric imperfections, residual stresses, and the adopted constitutive representation. Accordingly, the present finite element model is not regarded as quantitatively validated for ultimate-load prediction. The numerical results are retained primarily as a qualitative aid for interpreting deformation patterns, stress redistribution, and instability mechanisms. The von Mises stresses in the web and the displacement in the X-direction obtained from the finite element analysis are also shown in Figure 11, which illustrates the stress concentration around the opening and demonstrates how the retrofit techniques redistribute stresses and reduce localized effects. The figure shows the results for the control specimen BC and control specimen with additional stiffeners BC_TS. The finite element results provide various responses compared with the experimental result, since the smooth response expected numerically does not match the experimental one, which might be attributed to the effect of buckling on the deflection during the test. For specimens without openings, Figure 10a shows that the deflections of BC specimens against an ultimate load of 121 kN were about 3.47 and 2.8 mm according to the experimental test and numerical analysis, respectively, with a percentage difference of about −20%. Meanwhile, the deflections of the BC_TS specimen against an ultimate load of 149 kN were about 2.01 and 2.11 mm according to the experimental test and numerical analysis, respectively, with a percentage difference of about 5%. For specimens with an opening, Figure 10b shows that the deflections of the BO specimen against an ultimate load of 69 kN were about 2.0 and 1.5 mm according to the experimental test and numerical analysis, respectively, with a percentage difference of about −25%. Meanwhile, the deflections of the BO_TS specimen against an ultimate load of 120.2 kN were about 1.22 and 1.68 mm according to the experimental test and numerical analysis, respectively, with a percentage difference of about 38%. The high difference between the finite element and experimental model with an opening can be explained by considering the mode of failure obtained during the test, since irregular buckling for specimens with an opening was observed. This phenomenon cannot be shown by drawing or tracing the deflection of a certain node in the numerical analysis model. The comparison also demonstrates that the numerical predictions are strongly influenced by the adopted post-yield tangent modulus because the tested specimens failed primarily due to instability and web buckling rather than by extensive plastic yielding. The observed sensitivity confirms that the tangent modulus is one of the governing parameters in the adopted constitutive model and should be selected with appropriate engineering judgment when conducting nonlinear finite element simulations. However, the stress distribution shown in Figure 11 gives a better understanding of the behavior of the beam, which clearly shows the stress intensity obtained from the applied load. Figure 11a,c,g show that stress concentration near the applied load points and supports is obtained, which leads to distortion shown in Figure 11b,d,h. Figure 11e clearly depicts a high-stress concentration surrounding the opening, especially near the top corners, with slight differences. The results shown in Figure 11 indicated that the stresses in the web were less than the yield stress of the steel plate, indicating that yielding had not become widespread in the web at the loading stage illustrated. The numerical stress and deformation patterns are consistent with instability-dominated behavior rather than widespread material yielding. The expected failure is due to the instability of the member casing, excessive buckling, or deflection beyond the limits. The extrapolation of the rehabilitation process experimentally adopted by adding two horizontal stiffeners at the bottom and top of the opening provides good behavior. It was clearly shown that stresses rose to 195.7 MPa (Figure 11i), which means that the material reaches stages nearest to the yield compared with the other models. The cost analysis of rehabilitations compared with the remanufacturing and setting of a new beam can be explained in Table 8. The cost evaluation presented herein is intended to provide a relative comparison between the investigated rehabilitation techniques rather than a detailed economic assessment. Representative unit prices for structural steel and fabrication were adopted for comparison purposes only. Because material prices, fabrication costs, and labor rates vary with geographic location, market conditions, and project requirements, the absolute values reported in this study should not be interpreted as universally applicable. Instead, the comparison is intended to illustrate the relative cost-effectiveness of the investigated rehabilitation alternatives under consistent assumptions. The cost estimation depends on a price of steel of about $800 with manufacturing and installation, while the cost of rehabilitation using four stiffeners depends on a price of steel of about $1000 (since special techniques are required and the scaffold cast required to work in the field make it more expensive; the steel weight of the patch is ignored because it approximately represents the exact weight of the original section). The estimated rehabilitation cost was approximately 13.7% of the cost of installing a new beam, based on the assumptions adopted in Table 8. In general, the testing of the retrofitted specimens clearly showed the effect of using the patch plate technique and stiffeners for treating the opening, as summarized in Figure 12, which shows the effectiveness of the investigated rehabilitation techniques and confirms that the combined use of patch and stiffeners provides the best overall performance. Finally, a comparison between the present investigation and selected previous studies is summarized in Table 9. The main advance of the present work is the investigation of practical rehabilitation methods for accidental openings in slender-web bridge girders using welded steel patch plates and transverse stiffeners. The main advance of the present work is the investigation of a practical repair method for accidental openings in slender-web bridge girders using welded steel patch plates. Most previous studies focused on planned opening, CFRP strengthening, or numerical parametric studies. The present study provides experimental evidence that welded patch plates can partially restore the lost capacity, while combining patch plates with stiffeners provides the most effective rehabilitation performance. The finite element model exhibited differences from the experimental ultimate loads because of the idealized modeling assumptions discussed previously. A complete recalibration and revalidation of the constitutive model using experimentally determined post-yield hardening parameters was beyond the scope of the present study and is recommended for future work to improve the quantitative predictive capability of the numerical model. One limitation of the present experimental program is that only one specimen was tested for each rehabilitation configuration. Consequently, the study focuses on identifying comparative structural trends rather than establishing statistical variability. The experimental observations were complemented by nonlinear finite element analyses used to qualitatively examine the observed deformation and instability mechanisms. Nevertheless, additional repeated experiments are recommended in future studies to quantify the variability and statistical significance of the proposed rehabilitation techniques. Previous studies have demonstrated that geometric imperfections and web out-of-flatness can significantly influence the buckling response and strength of slender plate-girder webs [26,27]. In the present numerical model, welding-induced residual stresses, initial geometric imperfections, and fabrication-related imperfections were not explicitly incorporated. This limitation may contribute to discrepancies between the experimental and numerical responses. Future studies should incorporate these effects, together with additional experimental validation, to improve the quantitative prediction of the ultimate strength of rehabilitated slender-web steel girders. Future work should consider these factors together with additional experimental validation to improve the quantitative prediction of the ultimate strength of rehabilitated slender-web steel girders. Because only one representative specimen was tested for each rehabilitation configuration, the reported differences between specimens should be interpreted as observed experimental trends rather than statistically significant differences, particularly where the percentage differences are relatively small. Furthermore, local strain measurements around the opening and rehabilitation details were beyond the scope of the present study and are recommended for future investigations to better characterize local stress concentrations and buckling mechanisms. It should also be noted that all specimens were tested without lateral restraint under identical boundary conditions. Consequently, the observed behavior reflects the combined influence of the web opening and global lateral–torsional buckling for the adopted test configuration, and the conclusions should not be directly extended to laterally restrained or composite bridge girders.

Table 7. Ultimate load, ultimate deflection, and ultimate lateral displacement: finite element and experimental results.

No.	Designation	Exp. Pu kN	F.E. Pu kN	Exp. Defl. Ult. mm	F.E. Defl at Exp. Ult. Value mm	Defl. % Diff.	F.E. Pu kN Et = 8000	Difference in Pu at Et = 8000 MPa (%)	F.E. Defl at Exp. Ult. Value mm Et = 8000
1	BC	121.2	172.5	3.47	2.8	−19	49.85	−58.9	---
2	BC_TS	149.1	199.5	2.01	2.11	5	142.42	−4.5	---
3	BO	69.6	139.15	3.83	2.6	−32	32.5	−53.3	---
4	BO_TS	120.2	132.98	1.22	1.68	38	122.4	+1.8	6.0

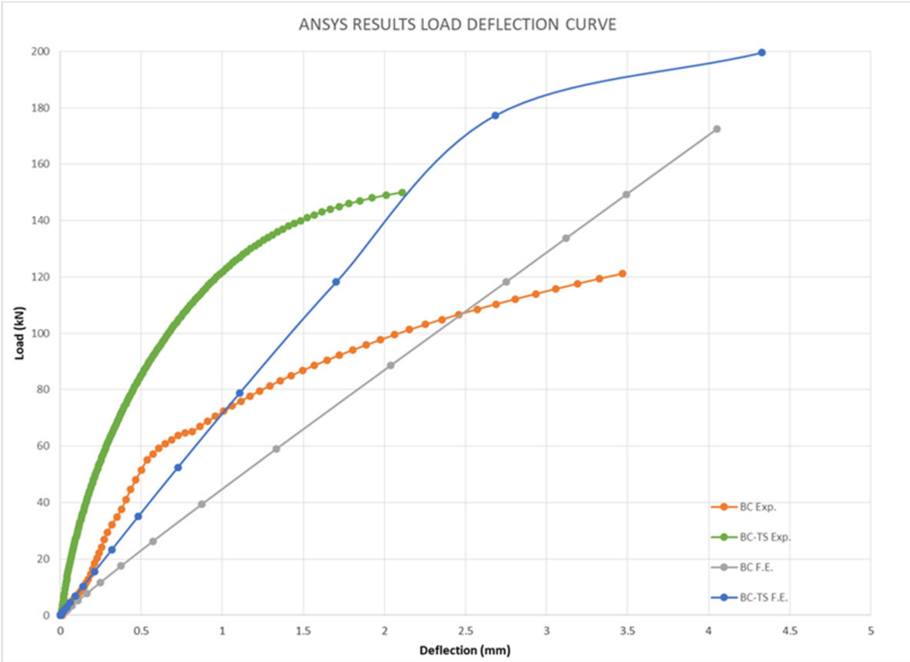

(**a**)

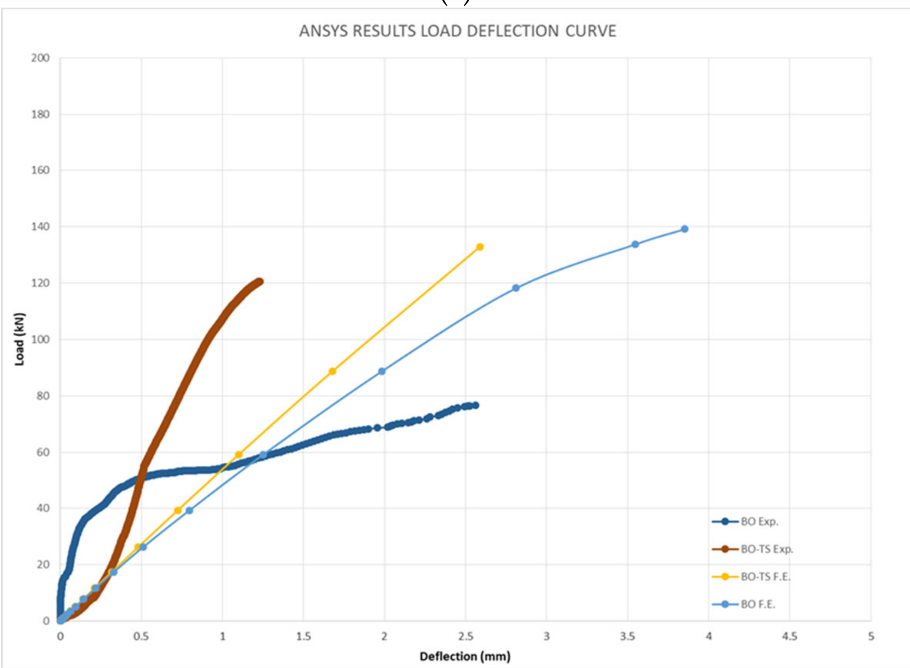

(**b**)

Figure 10. *Cont.*

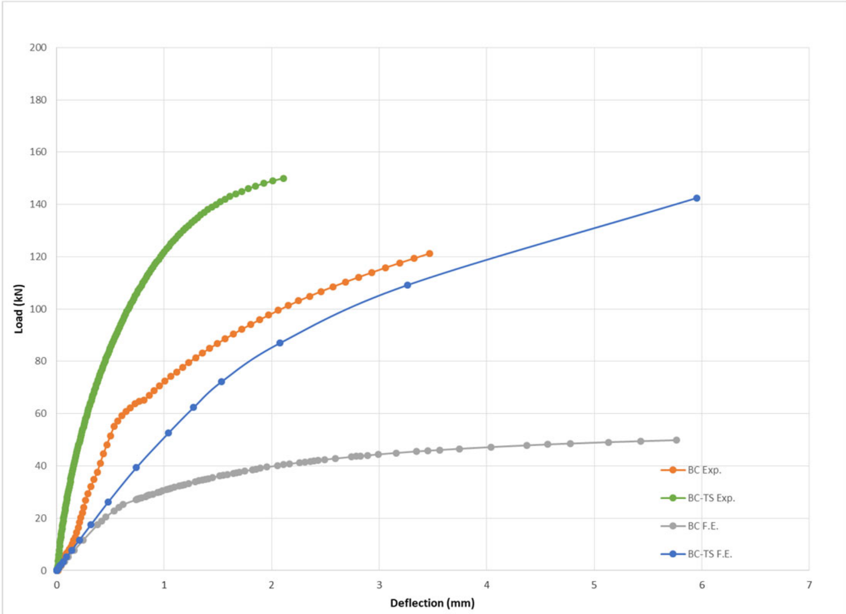

(c)

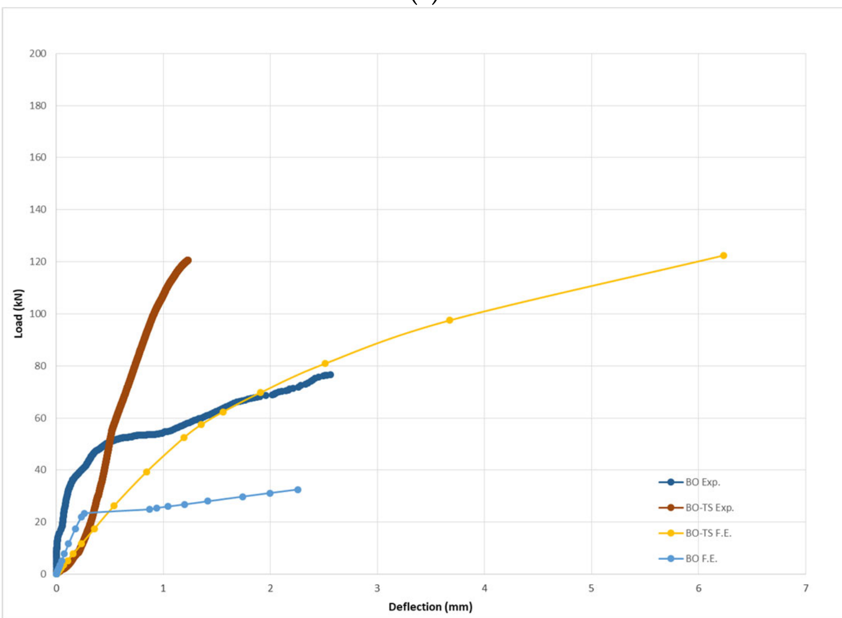

(d)

Figure 10. Load–deflection curves from finite element and experimental tests. (**a**) Sensitivity analysis for specimens without openings (Et = 120,000 MPa; calibration case). (**b**) Sensitivity analysis for specimens with openings (Et = 120,000 MPa; calibration case). (**c**) Reference-model response for specimens without openings (Et = 8000 MPa). (**d**) Reference-model response for specimens with openings (Et = 8000 MPa).

Table 8. Cost estimation for rehabilitation of steel beams compared with reconstruction.

Item	Value	Unit	Item	Value	Unit
No of stiffeners	4		Beam length	1800	mm
Stiffener length	800	mm	Flange width	300	mm
Stiffener width	140	mm	Flange thickness	10	mm
Stiffener thickness	4	mm	Web thickness	4	mm
Steel density	7.86	ton/m^3	Web height	800	mm

Table 8. *Cont.*

Item	Value	Unit	Item	Value	Unit
Stiffener steel volume	1,792,000	mm^3	Steel density	7.86	ton/m^3
Stiffener steel weight	14.08512	kg	Section area	9120	mm^2
			Beam steel volume	16,416,000	mm^3
			Stiffener steel weight	129.03	kg
Steel and manufacturing cost	1000	$ per ton	Steel and manufacturing cost	800	$ per ton
Cost for section 1.8 m	14.09	$	Cost for section 1.8 m	103.22	$
Cost for section/m	7.8	$ per meter	Cost for section/m	57.34	$ per meter
Percentage of rehabilitation cost comparing with new beam cost = 7.8/57.34=				13.7	%

Table 9. Comparison of the present study with selected previous studies on steel beams with web openings and strengthening techniques.

Study	Beam Condition	Strengthening Method	Main Finding
Abbas, (2023 [6])	Steel I beam with different web opening	NO repair	Opening reduced capacity depending on shape and size
Silwal et al., (2024 [12])	Steel beams with corrosion/web opening	CFRP	CFRP restored part of lost capacity
Al-Sultan and Al-Rifaie, (2024 [13])	Steel beams with large web opening	Parametric FE study	Opening size/location-controlled failure behavior
Present study	Slender-web girder with accidental opening	Welded patch plate	Patch plates increased strength by 22% to 26%
Present study	Slender-web girder with accidental opening	Vertical stiffeners	Stiffeners increased strength by 73%
Present study	Slender-web girder with accidental opening	Patch plates + stiffeners	Combined repair increased strength by 101–123%

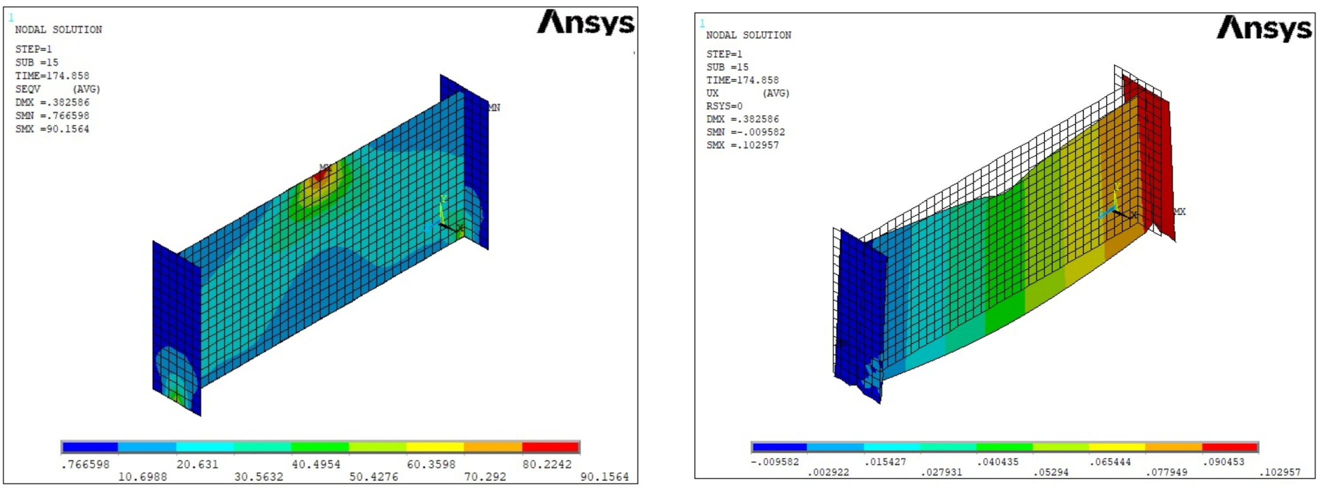

(**a**) (**b**)

Figure 11. *Cont.*

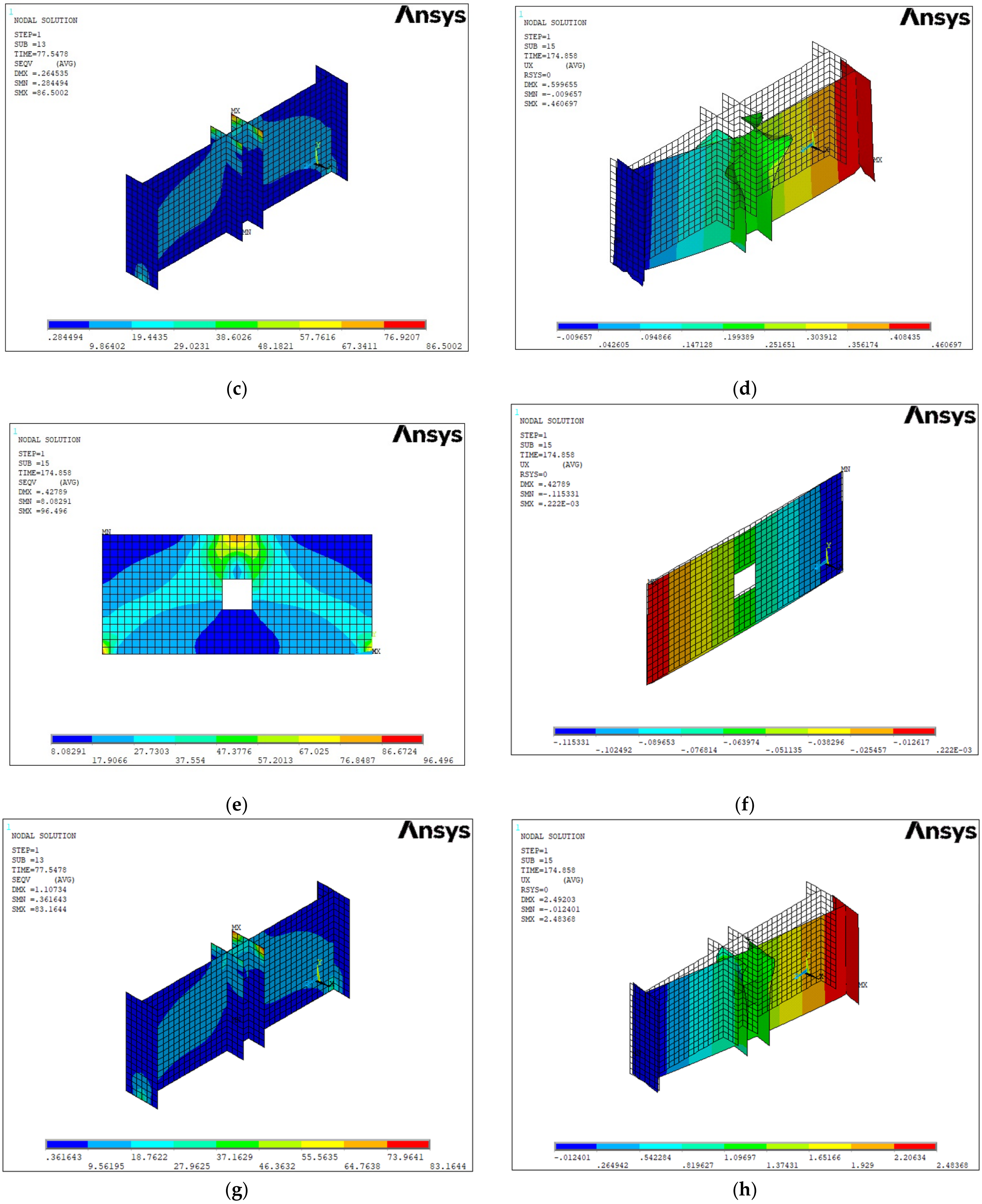

Figure 11. *Cont.*

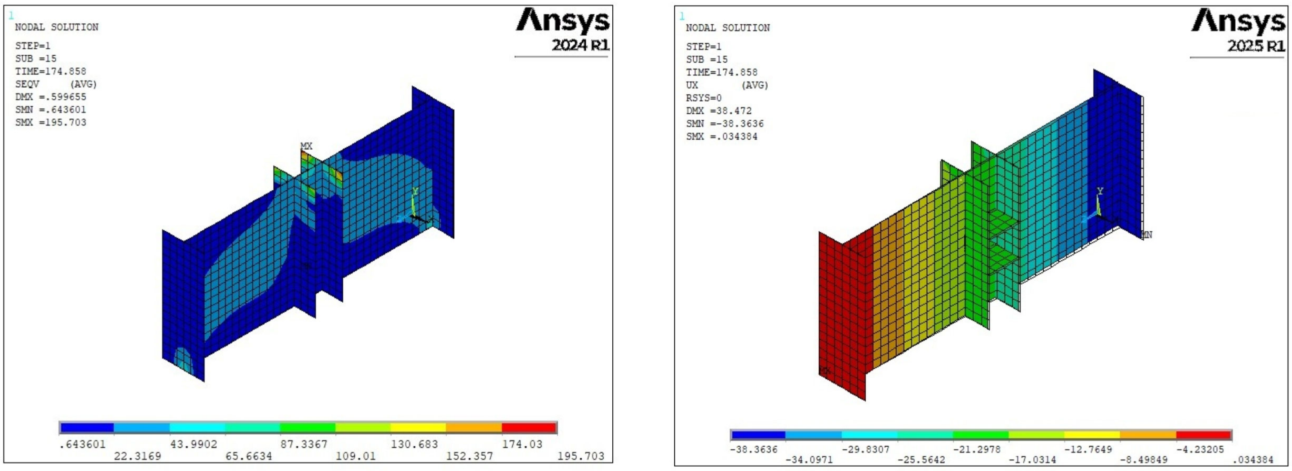

(i) (j)

Figure 11. The von Mises stresses in web and X-displacement t obtained from finite element analysis. (**a**) BC von Mises in web. (**b**) BC X-displacement in web. (**c**) BC_TS von Mises in web. (**d**) BC_TS X-displacement in web. (**e**) BO von Mises in web. (**f**) BO X-displacement t in web. (**g**) BO_TS von Mises in web. (**h**) BO_TS X-displacement t in web. (**i**) BO_TS + additional horizontal stiffeners' von Mises in web. (**j**) BO_TS + additional horizontal stiffeners' X-displacement t in web.

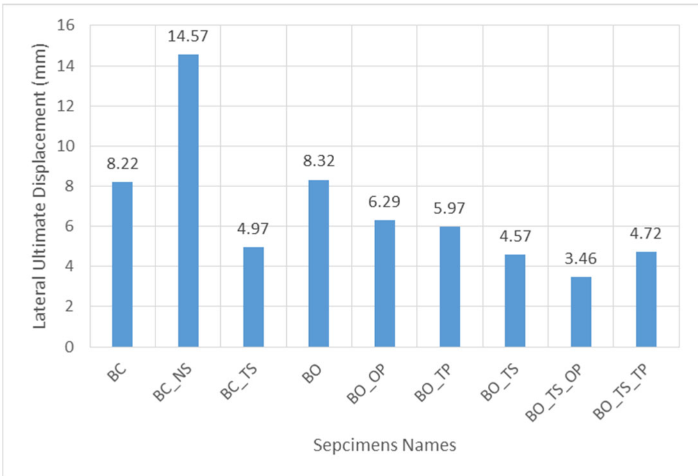

(**a**)

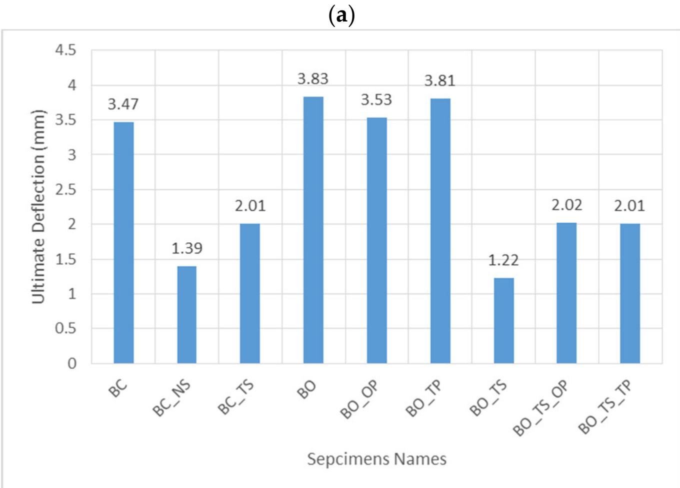

(**b**)

Figure 12. *Cont.*

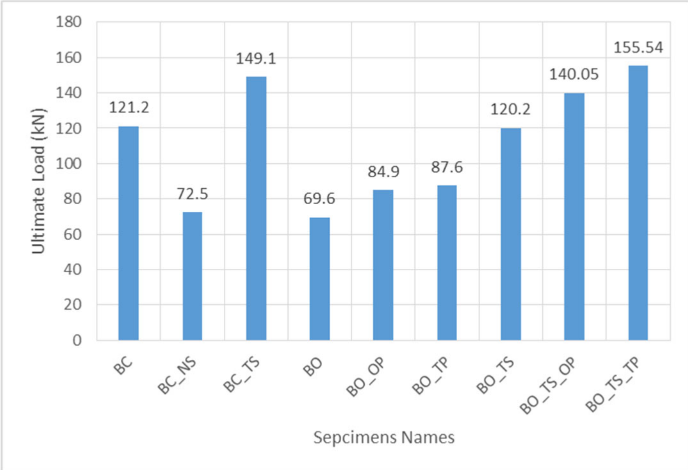

(**c**)

Figure 12. Variation in lateral displacement, deflection, and ultimate load for the adopted groups. (**a**) Variation in lateral displacement at ultimate deflection. (**b**) Variation in deflection displacement at ultimate deflection. (**c**) Variation in ultimate loads.

7. Conclusions and Recommendations

The conclusions presented in this study are limited to the tested conditions, namely, a single opening size, rectangular opening geometry, opening location, and monotonic static loading of non-composite welded steel I-girders under simply supported boundary conditions. The effects of fatigue loading, irregular corrosion or damage patterns, composite deck action, and actual bridge boundary conditions were not considered and should be investigated in future studies. Based on the experimental and numerical investigation of slender-web steel girders with accidental web openings, the following conclusions can be drawn:

- The experimental observations confirmed that the investigated rehabilitation techniques differ significantly in their effectiveness. Among the investigated methods, transverse stiffeners were more effective than welded patch plates alone, while the combined use of patch plates and transverse stiffeners provided the most efficient rehabilitation strategy by restoring load transfer and improving web stability.
- The presence of the accidental web opening significantly reduced the structural performance of the slender-web girder by interrupting the natural shear transfer mechanism and accelerating local web buckling.
- Welded patch plates partially restored the interrupted load path around the opening and provided an effective, practical rehabilitation method. However, patch plates alone could not fully suppress web instability.
- Transverse stiffeners were the most effective individual rehabilitation technique because they restrained local web buckling and increased the out-of-plane stiffness of the web panel. Consequently, the investigated specimens exhibited an increase in ultimate strength, together with substantially lower deflections at their respective ultimate loads.
- The combined use of welded patch plates and transverse stiffeners provided the highest structural efficiency by increasing the ultimate strength and significantly improving the stability of the girder by simultaneously restoring the interrupted load path and suppressing web instability. This rehabilitation strategy is therefore recommended for severely damaged slender-web steel girders requiring substantial strength recovery.

https://doi.org/10.3390/jcs10080429

- The dominant failure mode for all specimens was web buckling and global instability, rather than material yielding or weld failure.
- The FE model provides complementary numerical insight into the observed experimental behavior. Although some quantitative differences in ultimate load were observed because of idealized modeling assumptions, the numerical model proved suitable for evaluating the comparative effectiveness of the investigated rehabilitation techniques.
- The findings are applicable primarily to the local rehabilitation of damaged steel girders. Full-scale bridge applications should additionally consider composite action, fatigue, corrosion, service loading, and actual boundary conditions.
- This study contributes experimental and numerical evidence regarding practical rehabilitation techniques for accidental web openings in slender-web steel bridge girders and provides guidance for selecting effective strengthening strategies.

The present study has several limitations. Only one specimen was tested for each rehabilitation configuration; therefore, the experimental program was intended to identify comparative structural trends rather than establish statistical variability. Future research should include repeated experimental testing of each rehabilitation configuration to quantify statistical variability, cyclic and fatigue loading tests to evaluate long-term structural performance, full-scale bridge girder validation under realistic service conditions, investigation of additional rehabilitation configurations, and enhanced numerical models incorporating fabrication effects to improve the quantitative prediction of rehabilitated slender-web steel girders.

Author Contributions: Conceptualization, O.A.S. and S.Y.A.; methodology, S.Y.K.A.-D.; software, S.Y.K.A.-D.; validation, K.A.I., S.Y.A. and M.H.S.; formal analysis, K.A.I.; investigation, M.H.S.; resources, O.A.S.; data curation, K.A.I.; writing—original draft preparation, S.Y.K.A.-D.; writing—review and editing, S.Y.A.; visualization, S.Y.K.A.-D.; supervision, S.Y.K.A.-D.; project administration, O.A.S.; funding acquisition, K.A.I. All authors have read and agreed to the published version of the manuscript.

Funding: This research received no external funding.

Data Availability Statement: The experimental and numerical data used to support the finding of this study are available from the corresponding author upon reasonable request.

Acknowledgments: The authors wish to thank the staff of the Civil Engineering Department—College of Engineering at the University of Mosul for their cooperation in conducting the tests in the Material Engineering Laboratory.

Conflicts of Interest: The authors declare no conflicts of interest.

References

1. Al-Darzi, S.Y.K.; Ai Rong, C. Development of Hybrid Bridges: State of Arts and Conceptual Design. *J. Appl. Sci.* **2006**, *6*, 2799–2803. [CrossRef]
2. Fang, C.; Yam, M.C.H.; Lam, A.C.C.; Ke, K. Reinforcing strategies for double-coped beams against local web buckling. *Eng. Struct.* **2017**, *152*, 736–749. [CrossRef]
3. Galambos, T.V. *Guide to Stability Design Criteria for Metal Structures*, 5th ed.; John Wiley & Sons: Hoboken, NJ, USA, 1998. Available online: https://books.google.se/books/about/Guide_to_Stability_Design_Criteria_for_M.html?id=W_a0-8wiHdwC&redir_esc=y (accessed on 28 June 2026).
4. Jasim, W.A.; Allawi, A.A.; Ali Oukaili, N.K. Effect of Size and Location of Square Web Openings on the Entire Behavior of Reinforced Concrete Deep Beams. *Civ. Eng. J.* **2019**, *5*, 209–226. [CrossRef]
5. Al-Thabhawee, H.W.; Al-Kannoon, M.A. Experimental Study of the Behaviour and Failure Modes of Tapered Castellated Steel Beams. *Open Eng.* **2022**, *12*, 245–253. [CrossRef]
6. Abbas, J.L. Behaviour of Steel I Beams with Web Openings. *Civ. Eng. J.* **2023**, *9*, 596–617. [CrossRef]
7. Morkhade, S.G.; Gupta, L.M. Critical Study of Steel Beams with Web Openings. *Aust. J. Struct. Eng.* **2022**, *24*, 24–35. [CrossRef]

8. Heidarpour, A.; Bradford, M.A. Local Buckling and Slenderness Limits for Steel Webs Under Combined Bending, Compression and shear at Elevated Temperature. *Thin-Walled Struct.* **2008**, *46*, 128–146. [CrossRef]
9. Attiya, M.A.; Uraiyer, F.A.; Zainul-Abideen, A.Y.A. Rehabilitation of Reinforced Concrete Deep Beams by Near–Surface-Mounted Steel Reinforcement. *Open Eng.* **2023**, *13*, 20220473. [CrossRef]
10. Li, B.; Yang, Q.S.; Yang, N. An Investigation on Aseismic Connection with Opening in Beam Web in Steel Moment Frames. *Adv. Struct. Eng.* **2011**, *14*, 575–587. [CrossRef]
11. Jianga, Z.Q.; Kanga, Y.T.; Liu, X.C.; Cheng, K.K.; Chen, X. Experimental study of an earthquake-resilient prefabricated opening-web steel channel beam-to-column joint with flange cover plates. *Eng. Struct.* **2020**, *221*, 111054. [CrossRef]
12. Silwal, P.K.; Parvin, A.; Alhusban, M. Numerical Investigation on Strengthening of Steel Beams for Corrosion Damage or Web Openings Using Carbon Fiber Reinforced Polymer Sheets. *Buildings* **2024**, *14*, 1069. [CrossRef]
13. Al-Sultan, M.J.; Al-Rifaie, A. Numerical Study on the Impact Response of Steel Beams with Large Web Opening: Investigating Key Parameters. *Math. Model. Eng. Probl. IIETA* **2024**, *11*, 619–630. [CrossRef]
14. Ferreira, F.P.V.; Shamass, R.; Santos, L.F.P.; Tsavdaridis, K.D.; Limbachiya, V. Web-post buckling resistance calculation of perforated high-strength steel beams with elliptically-based web openings for EC3. *Structures* **2023**, *55*, 245–262. [CrossRef]
15. Jia, L.; Li, Q.; Ji, W.; Chen, C.; Du, J.; Geng, K. Influence of the Local Buckling of Web on the Bearing Capacity of the Castellated Beam/Composite Beam Under Pure bending. *Structures* **2024**, *63*, 106358. [CrossRef]
16. Liang, M.L.M.; Ma, Q.; Wang, P.; Ma, C. Web-post Buckling of Bolted Castellated Steel Beam with Octagonal Web Opening. *J. Constr. Steel Res.* **2020**, *164*, 105794. [CrossRef]
17. Salih, O.A.; Al-Saffar, N.A.H.; Al-Darzi, S.Y.K. Rehabilitation of the Second and Third Spans of the Steel Frame of Mosul's Second Bridge. *Case Stud. Constr. Mater.* **2023**, *17*, e01499. [CrossRef]
18. Shamass, R.; Ferreira, F.P.V.; Limbachiya, L.F.P.S.; Tsavdaridis, K.D. Web-Post Buckling Prediction Resistance of Steel Beams with Elliptically—Based Web Openings Using Artificial Neural Network (ANN). *Thin-Walled Struct.* **2022**, *180*, 109959. [CrossRef]
19. *ASTM A36/A36M-05*; Standard Specification for Carbon Structural Steel. ASTM International: West Conshohocken, PA, USA, 2005. Available online: https://store.astm.org/a0036_a0036m-05.html (accessed on 10 August 2026).
20. *ISO/IEC 17025:2017*; General Requirements for the Competence of Testing and Calibration Laboratories, Edition 3. ISO/IEC: Geneva, Switzerland, 2017.
21. *ANSI/AISC 360-16*; Specification for Structural Steel Buildings. American Institute of Steel Construction: Chicago, IL, USA, 2016. Available online: https://www.aisc.org/aisc/publications/current-standards/aisc-360/ (accessed on 10 August 2026).
22. Williams, A. *Steel Structures Design ASD/LRFD*; McGraw Hill Publishing: New York, NY, USA, 2011; p. 573.
23. Thompson, M.K.; Thompson, J.M. *ANSYS Mechanical APDL for Finite Element Analysis*, 1st ed.; Butterworth-Heinemann Elsevier: Oxford, UK, 2017; p. 438.
24. Kohnke, P. *ANSYS Mechanical APDL Theory Reference*; ANSYS Inc.: Canonsburg, PA, USA, 2013; p. 988. Available online: https://ansyshelp.ansys.com/public/Views/Secured/corp/v252/en/pdf/ANSYS_Mechanical_APDL_Theory_Reference.pdf (accessed on 28 June 2026).
25. Moaveni, S. *Finite Element Analysis Theory and Application with ANSYS*; PRENTICE HALL: Hoboken, NJ, USA, 1999; p. 527. Available online: http://ftp.demec.ufpr.br/disciplinas/TM738/Livros/Finite%20Element%20Analysis,%20Theory%20and%20application%20with%20ANSYS,%20.pdf (accessed on 28 June 2026).
26. Graciano, C.; Chacón, R.; Mirambell, E.; Real, E. Imperfection sensitivity of plate girder webs subjected to patch loading. *J. Constr. Steel Res.* **2011**, *67*, 1128–1133. [CrossRef]
27. Masungi, P.M.; Garlock, M.E.M.; Augustyn, K.E.; Quiel, S.E. Out-of-flatness of steel plate girder webs, Part II: Shear strength and behavior. *J. Constr. Steel Res.* **2024**, *219*, 108788. [CrossRef]

Disclaimer/Publisher's Note: The statements, opinions and data contained in all publications are solely those of the individual author(s) and contributor(s) and not of MDPI and/or the editor(s). MDPI and/or the editor(s) disclaim responsibility for any injury to people or property resulting from any ideas, methods, instructions or products referred to in the content.